Food Chemistry 365 (2021) 130457

Contents lists available at ScienceDirect

Food Chemistry

journal homepage: www.elsevier.com/locate/foodchem

Effect of processing and storage on the volatile profile of sugarcane honey: A four-year study

Pedro Silva [a], Jorge Freitas [a], Fernando M. Nunes [b], José S. Câmara [a,c,*]

[a] CQM-Centro de Química da Madeira, Universidade da Madeira, Campus da Penteada, 9020-105 Funchal, Portugal
[b] CQ-VR, Centro de Química – Vila Real, Food and Wine Chemistry Lab., Departamento de Química, Universidade de Trás-os-Montes e Alto Douro, 5001- 801 Vila Real, Portugal
[c] Departamento de Química, Faculdade de Ciências Exactas e Engenharia, Universidade da Madeira, Campus da Penteada, 9020-105 Funchal, Portugal

ARTICLE INFO

Keywords:
Sugarcane honey
Making process
Storage
Volatile profile
Authenticity

ABSTRACT

Sugarcane honey (SCH) is a syrup from Madeira Island recognized by its unique and excellent aroma, associated to volatile organic compounds (VOCs) generated during the well-defined five stages of its traditional making process. The establishment of volatile profile throughout all SCH-making stages during four years, allowed the evaluation of the influence of each stage in the typical characterisitcs of SCH. One hundred eighthy seven VOCs were identified, being associated to several origins and formation pathways. VOCs formed during stage 1 and 2 were originate from raw material, and its oxidation (i.e. enzymatic browning) and thermal degradation (i.e. lipid oxidation, Maillard reactions, Strecker degradation). In stage 3 and 4, the caramelization and melanoidin degradation also occurred, while in stage 5, the thermal degradation continues, followed by microbial activity. Chemometric analysis allowed to identify 35 VOCs as potential markers for processing control by the producers and as guarantee of the typicality and authenticity of SCH. Based on the obtained results, we propose for the first time an innovative schematic diagram explaining the potential reactions and pathways for VOCs formation during the different steps of the SCH production.

1. Introduction

The sugarcane honey (SCH), known as "*mel-de-cana*", is a crystalline black syrup produced by thermal processing of the juice from sugarcane (SC) stalks (*Saccharum officinarum L.*) cultivated under mild climate conditions in Madeira Island, Portugal. SCH is a regional product of excellence, worldwide recognized by its typical and unique aroma, being consumed in fresh or used as a main ingredient in traditional pastry and confectionery, as well in sauces for cooking meat, fish and salads or even for medicinal purposes. SCH is a syrup without any additive, colorant or preservative, being naturally rich in carbohydrates, minerals (Fe, Ca, Mg and Cu), vitamins (niacin, riboflavin and thiamin), antioxidants (flavonoids and non-flavonoids) and fibers (Silva et al., 2017; Silva, Silva, Perestrelo, Nunes, & Câmara, 2018).

The traditional making process of SCH is a true form of engineering and art, being based on five main stages: (i) S1 - starts with the placement of SC stalks in a grinder, where the juice, also known as "*guarapa*", is extracted by mechanical pressing; (ii) S2 - the fresh juice is directly conducted to a first heated filtering process with a nylon membrane at 80 °C; (iii) S3 - the filtered SC juice is heated up to 100 °C for 24 h into an evaporator to produce a primary and dark brown syrup, wherein is led to a second filtering process; (iv) S4 - the primary syrup is again placed into an evaporator for 10 h with a temperature up to 120 °C, to continue the thermal process and evaporation of the remaining water, being again filtered to ensure a flawless rigor of final product, a viscous and crystalline black syrup; (v) S5 - finally, the syrup is storage in a reservoir at 20 °C for 6 months, where it cools down naturally.

The typical and unique aroma of SCH is strongly influenced by the presence of volatile organic compounds (VOCs) that arise from its raw material, traditional processing and storage (Silva et al., 2017). Although some VOCs can be originated from the SC raw material, most are formed by a wide variety of reactions that occur during SCH making process, including the well-known browning reactions (BRs) (Silva et al., 2017). BRs can be divided into two main types of reactions, enzymatic (EBRs) and non-enzymatic (NEBRs). EBRs are caused by the activity of enzymes on the polyphenols in the SC juice

* Corresponding author at: CQM-Centro de Química da Madeira, Universidade da Madeira, Campus da Penteada, 9020-105 Funchal, Portugal.
E-mail address: jsc@staff.uma.pt (J.S. Câmara).

https://doi.org/10.1016/j.foodchem.2021.130457
Received 25 March 2021; Received in revised form 21 June 2021; Accepted 22 June 2021
Available online 1 July 2021

during stalk pressing, where can promote the formation of VOCs in an indirect way through posterior reactions of its products, such as quinones, with amino acids. On the other hand, the NEBRs are probably the main source of VOCs in thermal processed foods, encompassing a complex set of chemical reactions where a large number of food components (i.e. sugars, amino acids, proteins, lipids, and vitamins) participate via multiple different pathways, originating a great diversity of VOCs (Gao et al., 2017; Göncüoğlu Taş & Gökmen, 2017). Particularly, the VOCs responsible for the unique aroma of SCH are mainly formed by Maillard reactions, Strecker degradation and caramelization (Silva et al., 2017). The high temperatures used during SCH processing and the large content of sugars in SC provide optimal conditions for these reactions. In addition, other NEBRs can also occur during SCH processing, namely the thermal degradation of lipids and L-ascorbic acid (Silva et al., 2017). Moreover, some NEBRs can also occur during storage in products with high sugar and free amino acids content, such as honey, jam and syrups (Santos-Zea et al., 2016). Additionally, some enzymes can react with several components (i.e. fatty acids, ascorbic acid, due to the disruption of plant tissues that occurs throughout the harvesting, crushing and pressing of SC stalks. Finally, the microbial activity can occur naturally by bacteria, fungi or yeast on the sugars during the period of harvest and transportation of SC to the factory, and also in the storage of the SCH, leading to formation of several VOCs (Thompson, 2009; Wang, Li, Yang, Ruan, & Sun, 2016). Thus, the exclusive use of SC cultivated on Madeira Island and the strict conditions used in traditional processing and storage can generate similarities in VOCs profile that potentially create a "fingerprint" of SCH, being a valuable strategy for establishment of its typicality and authenticity.

Consequently, the control and monitoring of the chemical composition during the food processing stages is crucial to ensure the expected and typical organoleptic properties (i.e. aroma, flavor and texture) of a particular food product in order to guarantee its quality, typicality and authenticity, as well its compliance with national legislation, international standards and consumer safety rules. In this context, solid-phase microextraction in headspace mode (HS-SPME) combined with gas chromatography-mass spectrometry (GC–MS) is, undoubtedly, the most popular method used for volatile profiling in Foodomics domain, being widely applied as an effective and usefull tool for monitoring of VOCs during the processing of food products, such as wine (Ubeda et al., 2019), soy sauce (Gao et al., 2010), green tea (Wang et al., 2016), coffee (Ishwarya & Anandharamakrishnan, 2015), vinegars (Ubeda et al., 2011), among others.

The aim of the current study is the monitoring of volatile profile during the five main stages of SCH processing (S1, S2, S3, S4 and S5) in a certified producer through four years (2015, 2016, 2017 and 2018) using the HS-SPME/GC–MS method previously developed, optimized and fully validated in our previous study (Silva et al., 2017). The chemometric analysis was performed according to the procedures developed in our previous studies (Silva et al., 2017, 2018), with some modifications. The data obtained from this study represents the first attempt to evaluate the volatile profile throughout all stages of SCH processing, providing a highly valuable information about the influence of raw material, effect of processing conditions (i.e. temperature, pH), impact of precursors (i.e. sugars, amino acids, lipids) and complexity of reactions involved (i.e. browning reactions and microbial activity). Moreover, this information can be useful for an optimization of SCH processing and storage, where the importance of each stage was evaluated. Likewise, the identification of VOCs markers allows the strict control of key stages by producers in order to achieve the typical organoleptic proprieties expected by consumers. Finally, this data represents a powerful platform to guarantee the typicality and authenticity of SCH, supporting its EU certification of geographical origin, namely the Protected Designation of Origin (PDO) and Protected Geographical Indication (PGI).

2. Materials and methods

2.1. Standards, reagents, materials and software

Sodium chloride was acquired from Panreac (Barcelona, Spain). The internal standard (IS), 4-heptanone, was purchased from Sigma-Aldrich (St. Louis, Missouri, USA). SPME holder for the manual sampling of SPME fiber and the fiber divinylbenzene/carboxen/polydimethylsiloxane (DVB/CAR/PDMS) with 50/30 μm film thickness were purchased from Supelco (Bellefonte, PA, USA). Ultrapure deionized water (H_2O), purified with a Milli-Q ultra-pure water system from Millipore (Massachusetts, USA). The MAXI MIX Vortex Mixer was acquired from Thermo Scientific (Massachusetts, USA). All data analysis and statistical processing were performed using the STATSOFT STATISTICA 12.0 (2013) software (Tulsa, USA).

2.2. Samples

Samples from all stages (S1, S2, S3, S4 and S5) of processing and storage of SCH were provided by the traditional and certified producer *Fábrica de Mel-de Cana do Ribeiro Sêco (FRS)*, Madeira Island, Portugal, in April 2015, 2016, 2017 and 2018, being stored under stable conditions (4 °C, in the dark). Identification (ID) replicate number, ID replicate code, ID sample code, ID stage code, processing year, processing stage description and producer name are presented in Supplementary Material (SM) Table 1.

2.3. Solid phase microextraction procedure

The SPME procedure used for VOCs extraction from SCH samples was based on our analytical method previously developed, optimized and validated (Silva et al., 2017). Briefly, all samples were daily diluted in the ratio 3:2 (w/v), where 15 g of sample was added to 10 mL of deionized water (H_2O) placed into a 50 mL PTFE centrifuge tube, being mechanical homogenized during 1 min and stored at 4 °C in aliquots of 5 mL. After, these aliquots were transferred to an 8 mL glass vial with 60 mg NaCl previously added, which was placed in a thermostatic bath at 30 °C for 5 min for sample temperature equilibrium. The SPME was performed in headspace mode (HS), where the fiber DVB/CAR/PDMS was attached to a manual SPME holder and exposed in the sample headspace during 60 min at 30 °C, under magnetic agitation (600 rpm). The VOCs extracted by SPME were thermally desorbed by the fiber direct insertion into GC injector at 250 °C, in splitless mode for 10 min. The fiber was daily conditioned for 15 min at 250 °C into GC injector to avoid contamination by unwanted interferents. Triplicate experiments were performed for all samples under analysis. Blank experiments were performed before the analysis of each sample, where the fiber was directly placed into GC injector without being subjected to any SPME extraction procedure.

2.4. Gas Chromatography-Mass spectrometry analysis

The analysis of extracted VOCs was carried on Agilent Technologies 6890 N Network gas chromatography system (Santa Clara, California, USA) equipped with a BP-20 fused silica capillary column with 60 m × 0.25 mm I.D. × 0.25 μm film thickness (SGE, Dortmund, Germany), and interfaced with an Agilent 5975 quadrupole inert mass selective detector (Santa Clara, California, USA). The employed protocol for column oven temperatures was: 40 °C for 2 min, then was increased at 0.25 °C min^{-1} until 45 °C with a 2 min hold, after was increased at 4 °C min^{-1} to 70 °C with a 2 min hold, was increased again at 3 °C min^{-1} to 130 °C with a 2 min hold, and finally, was increased at 3 °C min^{-1} to 220 °C, this final temperature was maintained during 7 min, for a total GC run time of 91.25 min. Column flow was constant at 1 mL min^{-1} using He carrier gas at a purity of 99.999% (Helium N60, Air Liquid, Portugal). The injection port was operated in the splitless mode and held at 250 °C. For the 5975

MS system, the operating temperatures of the transfer line, quadrupole and ionization source were 270, 150 and 230 °C respectively. Electron impact mass spectra was recorded at 70 eV ionization voltages and the ionization current was 10 μA. The electron multiplier was set to the auto tune procedure. The acquisitions were performed in scan mode (30–300 *m/z*). VOCs identification was based on visual interpretation of spectra through the Agilent MS ChemStation Software, and confirmed comparing each VOC mass spectra with the NIST14 Mass Spectral Library (2014), being successfully identified when a similarity threshold was higher than 75%. The total peak area values were obtained by target ion quantification protocol. The results are presented as relative peak areas (RPA), which were calculated by dividing the total peak area value of each VOC by the total peak area value of IS.

2.5. Chemometric analysis

The chemometric analysis procedure was performed according the previously developed procedures in our previous studies (Silva et al., 2017, 2018), being introduced some modifications based on the recommendations for analytical applications (Esteki et al., 2018; Lubes & Goodarzi, 2017). *One-way* ANOVA test was performed to determine the VOCs with statistically significant differences ($p < 0.05$) on its variance level between RPA values of samples obtained throughout all stages of SCH processing during 2015–2018 production years. Furthermore, individual *One-way* ANOVA tests were performed for S1-S2, S2-S3, S3-S4 and S4-S5 transitions. Principal component analysis (PCA) and partial least squares (PLS) analysis were performed on RPA values of VOCs dataset to achieve the preview of correlation structure of samples from all stages, being constructed according to the samples variance, without and with stage classification, respectively. A 7-fold cross-validation was performed. Linear discriminant analysis (LDA) was used as supervised pattern recognition method for variable selection in order to obtain a matrix composed by the lowest number of VOCs that lead to a correct classification of all samples for the group assignment (S1, S2, S3, S4 and S5). A backward selection method (*p* value of 0.05 to enter and remove) was used to determine the most predictive VOCs and remove the least predictive from analysis, being formed a classification structure according the canonical discriminant functions. A leave-one-out cross validation was performed. LDA is commonly suggested as an efficient method to reduce the dimensionality of large dimension matrix into a lower dimension matrix by removal of less predictive variables preserving the interclass separation (classification structure).(Esteki et al., 2018; Lubes & Goodarzi, 2017) A matrix reduction procedure was applied prior to LDA, where the matrix was reduced to 20% of initial dimension based on F-value from *One-way* ANOVA between all stage samples. Alternatively, a matrix reduction procedure based on the VIP scores from the PLS analysis was also applied. Thus, the 37 VOCs with higher F-Value and VIP score were selected, respectively. Finally, a second PLS analysis and hierarchical clustering analysis (HCA) were applied on RPA values of the most predictive VOCs. PLS based on dataset from the reduced matrix was performed to confirm the correlation structure between all samples when classified according to stage of SCH processing, and compare with structure obtained from previous PLS performed with all 187 VOCs. HCA was performed in order to determine the Euclidean linkage distances between all samples and achieve a visual measure of distance and linkage criterion between stages throughout SCH processing based only in the most predictive VOCs.

3. Results and discussion

3.1. Monitoring the volatile profile throughout the sugarcane honey processing

For the first time, in a four year study (2015–2018), the HS-SPME/GC–MS method was successfully applied to monitor the volatile profile during the traditional processing and storage of SCH. The ID number, retention time, main ions (*m/z*), target ion, match percent, IUPAC name, NIST database, abbreviation, CAS number, molecular formula and main chemical class of identified VOCs are described in SM Table 2. The mean relative peak areas (RPA) values and respective relative standard deviation (RSD) of identified VOCs in samples during SCH processing stages from 2015 to 2018 production years are described in SM Table 3. The mean, minimum and maximum values of RPA for identified VOCs in each SCH processing stage are summarized in SM Table 4. The typical GC–MS chromatograms for S1, S2, S3, S4 and S5 of SCH processing are presented in SM Fig. 1(A), (B), (C), (D) and (E), respectively. Chemically, the volatile profile during SCH processing varies greatly from stage to stage, where can be observed a high diversity of the number, chemical classes and RPA values of identified VOCs for each stage.

3.1.1. Number of identified volatile organic compounds

A total of 187 different VOCs were identified in samples from the five stages (S1-S5) of SCH processing between the years of 2015 and 2018. The number of identified VOCs for each stage were: 126 (S1), 136 (S2), 136 (S3), 136 (S4) and 149 (S5), wherein 93 VOCs (49.7%) are common to all stages. However, only 31 VOCs (16.6%) were identified in a specific stage: 11 (S1), 5 (S2) and 15 (S5). Curiously, only 51 (34.2%) of the 149 VOCs from S5, were identified on the SCH samples from the certified producer in our previous study (Silva et al., 2017). The increase in the number of VOCs identified may be due to the database update (NIST05 to NIST14), and mainly, due to the identification procedure used, where all the 187 VOCs were searched in all samples based on a stage-by-stage follow-up strategy. Moreover, off the all 187 VOCs, 103 (52.3%) were previously identified in others SC based-products, namely: 30 in juice, 42 in brown sugar, 31 in molasses, 18 in treacle, 64 in syrup, 38 in rum, 6 in infusions, and 6 in alcoholic-fermented beverage described as “SC wine”. This information and respective references are described in SM Table 5.

There, 92 VOCs (46.7%) have been previously identified in thermally processed SC products, such as syrups (Asikin et al., 2018; Chen et al., 2020; De Andrade et al., 2016; Ruiz-Matute, Soria, Sanz, & Martínez-Castro, 2010; Silva et al., 2017), molasses (Abe, Nakatani, Yamanishi, & Muraki, 1978; Franitza, Granvogl, & Schieberle, 2016; Quinn, Bernier, Geden, Hogsette, & Carlson, 2007), treacle (Edris, Murkovic, & Siegmund, 2007) and brown sugar (Asikin et al., 2016, 2014; Chen et al., 2020; Payet, Shum, Sing, & Smadja, 2005; Takahashi et al., 2016), wherein most of them were identified in S3, S4 and S5 of SCH processing. This is indicative of the influence of NEBRs in the volatile profile of SCH, particularly, the thermal degradation of SC components (i.e. sugars, amino acids). On the other hand, only 30 VOCs (15.2%) were identified in unprocessed products based on SC juice, mainly identified in S1 and S2, being potentially from SC plant biochemistry, and also from enzyme and microbial action on SC components (Chen et al., 2020; Sharma, Rautela, Sharma, Gahlot, & Koshy, 2015; Tokitomo, Kobayashi, & Yamanishi, 1984; Wang et al., 2020; Wang, Wang, Deng, Cai, & Chen, 2019; Yang, Wang, Yu, Zeng, & Sun, 2014). Interestingly, 40 VOCs (20.3%) were previously identified in SC alcoholic-fermented beverages, such as spirits, rum, and wine, being mainly identified in final SCH product (S5), suggesting a potential action of microorganisms during its storage (Cardeal & Marriott, 2009; Coelho et al., 2020; De Souza, Vásquez, Del Mastro, Acree, & Lavin, 2006; Franitza, Nicolotti, Granvogl, & Schieberle, 2018; Serafim, Pereira-Filho, & Franco, 2016; Tábua et al., 2020; Zacaroni, de Sales, Cardoso, Santiago, & Nelson, 2017).

3.1.2. Main volatile organic compounds

More than one hundred VOCs were identified for each stage of the SCH processing, where were obtained RPA ($\times 10^3$) values from 0.5 to 500000. Although the importance of each VOC to the volatile profile should not be measured only through its RPA value, this relative measure is vital to understand which are the main VOCs for each stage of SCH processing. The RPA values for the 20 main VOCs of S1, S2, S3, S4 and S5 are described in Fig. 1 (A), (B), (C), (D) and (E), respectively.

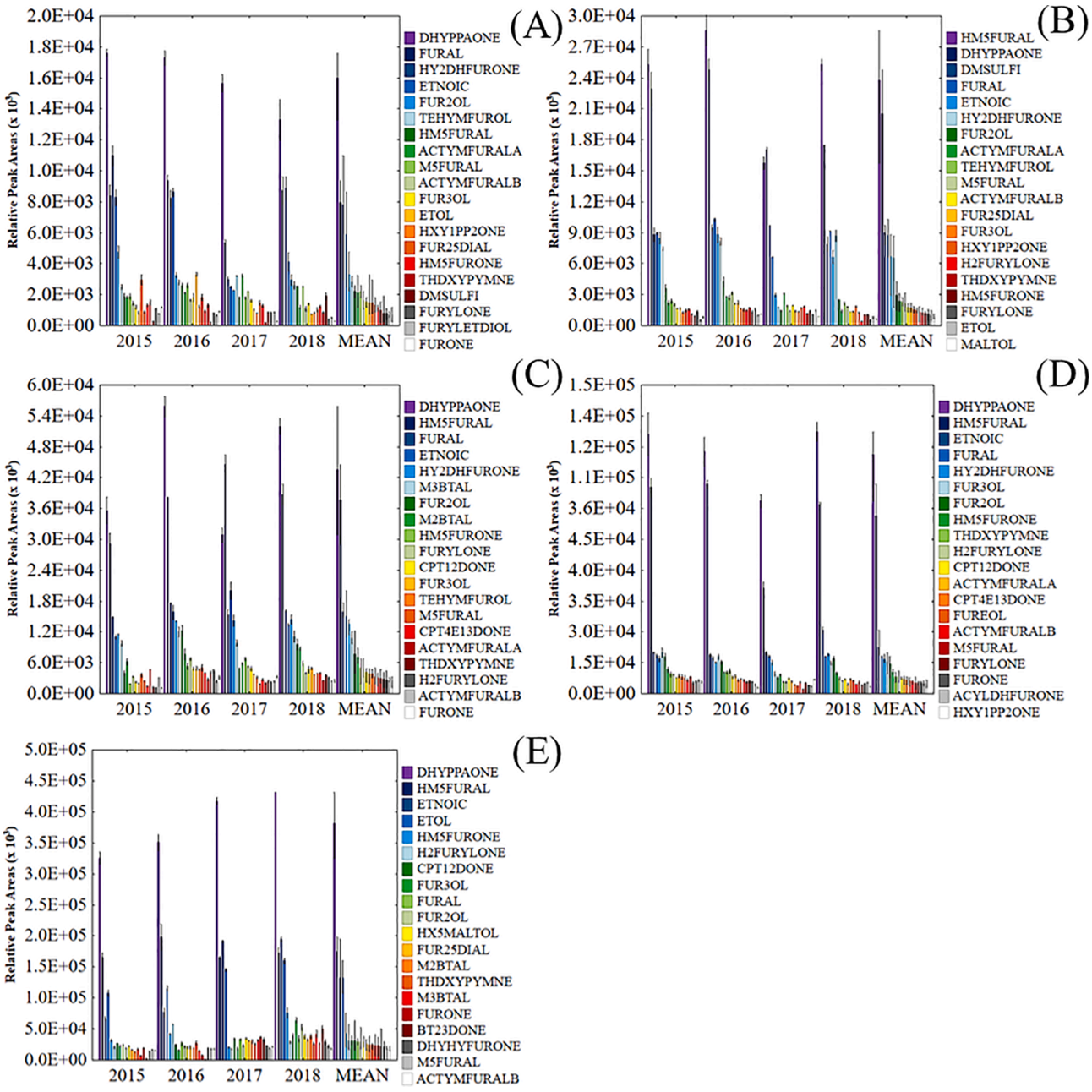

Fig. 1. The relative peak area values of the 20 main VOCs at different stages of SCH making: stage 1 (A), stage 2 (B), stage 3 (C), stage 4 (D) and stage 5 (E).

Through the analysis of the 20 main VOCs for each stage of SCH processing were found 32 different VOCs, where 10 were common to all stages, namely 1,3-dihydroxy-2-propanone (DHYPPAONE), furfural (FURAL), ethanoic acid (ETNOIC), 2-furanmethanol (FUR2OL), 5-(hydroxymethyl)-2-furfural (HM5FURAL), 5-methyl-furfural (M5FURAL), 5-acetoxymethyl-2-furfural B (ACTYMFURALB), 3-furanmethanol (FUR3OL), 5-(hydroxymethyl)-dihydro-2(3H)-furanone (HM5FURONE) and 2,4,6-trihydroxypyrimidine (THDXYPYMNE). On the contrary, eight were classified as main VOCs only in one stage, such as 1-(2-furanyl)-1,2-ethanediol (FURYLETDIOL) for S1, maltol (MALTOL) for S2, 5-Acetyl-Dihydro-2(3H)-Furanone (ACYLDHFURONE), furaneol (FUREOL) and 1-hydroxy-2-propanone (HXY1PP2ONE) for S4, and 5-hydroxy-maltol (HX5MALTOL), 2,3-butanedione (BT23DONE) and 4-hydroxy-dihydro-2(3H)-furanone (DHYHYFURONE) for S5. Although not all of these VOCs have been classified as main contributors in all stages, 30 main VOCs were positively identified in all stages, with exception of BT23DONE (S2, S3, S4 and S5) and HY5MALTOL (S3, S4 and S5).

As expected, most of the main VOCs appears to be strongly linked to the NEBRs, such as DHYPPAONE (main contributor in S1, S3, S4 and S5), HM5FURAL (main contributor in S2), FURAL, M5FURAL and FUR2OL (Silva et al., 2018; Stasiak-Rózńska & Płoska, 2018). However, some high contributors VOCs commonly associated with NEBRs, such as ETNOIC and dimethyl sulfide (DMSULFI), can also be formed by action of microorganisms (Deed et al., 2019; Sengun & Karabiyikli, 2011). Remarkably, others main VOCs appear to be non-related to NEBRs. For example, ETOL has only high contribution in S1 and S5, where its formation in SCH is probably from enzyme or microbial activity (Kanakaraju et al., 2020; Thompson, 2009).

3.1.3. *Chemical class classification of volatile organic compounds*

Throughout the five stages of SCH processing was possible to recognize an enormous diversity of chemical classes, being fundamental its classification to characterize the volatile profile of each stage. The

classification based on main chemical class of each VOC are described in SM Table 2. The summary of number of VOCs, RPA and TRPA values of main chemical classes identified in stage samples are summarized in SM Table 6. The contribution, RPA and % TRPA values, of each chemical class to volatile profile of all stages is presented in Fig. 2 (A) and (B), respectively.

A total number of 17 chemical classes were identified, namely alcohol (ALC), aldehyde (ALD), benzene (BNZ), benzofuran (BZF), carboxylic acid (CAC), ester (EST), ether (ETH), furan (FUR), hydrocarbon (HYD), indene (IND), ketone (KET), naphthalene (NPH), nitrogen (NIT), phenol (PHE), pyran (PYR), sulfur (SUL) and terpene/terpenoid (TER). The specific contribution of all chemical classes for each stage can be ordered according the mean TRPA values (2015, 2016, 2017 and 2018) in the following decreasing order: (S1) - FUR > KET > CAC > ALC > NIT > ALD > PYR > BNZ > SUL > EST > HYD > PHE > ETH > TER > BZF > NPH; (S2) - FUR > KET > SUL > CAC > NIT > ALC > PYR > ALD > BNZ > PHE > BZF > EST > TER > ETH > HYD > NPH; (S3) - FUR > KET > ALD > CAC > NIT > PYR > PHE > BNZ > EST > ALC > BZF > ETH > NPH > SUL > HYD > TER > IND; (S4) - FUR > KET > CAC > NIT > PYR > ALD > EST > BNZ > PHE > ALC > BZF > ETH > TER > HYD > SUL > NPH > IND; (S5) - FUR > KET > ALC > CAC > NIT > PYR > ALD > BNZ > EST > PHE > BZF > TER > ETH > SUL > NPH > IND > HYD.

VOCs from 16 of 17 chemical classes were identified in all stages of SCH processing, the exception was IND group (identified only in S3, S4 and S5). Furthermore, for the first time, IND-VOCs were identified in SC-based products, being the only class where none VOC was identified in our previous study with certified SCH samples (Silva et al., 2017), and also in SC based-products described in SM Table 5. Undoubtedly, VOCs from KET and FUR were the main contributors to volatile profile throughout all stages of SCH processing, being always higher than 20%. FUR had the larger contribution and higher number of VOCs (44) in all stages, being about 50% in the S1, S2, S3 and S5. The VOCs with more influence in FUR contribution were HM5FURAL, HM5FURONE, FUR3OL, FUR2OL and FURAL. KET was the secondary main contributor in all stages, presenting a balanced contribution during SCH processing, between 20 and 35%. 19 VOCs were assigned in KET, where the main contributor was DHYPPAONE, being followed by BT23DONE and 1,2-Cyclopentanedione (CPT12DONE). VOCs from ALD, CAC, NIT and PYR presented a reasonable contribution (>1%) during all stages, being more expressive in the last three stages for PYR and NIT. Regarding the dimension, the number of VOCs assigned to each class was: NIT (16), ALD (14), CAC (8) and PYR (5). The contribution of NIT was mainly influenced by THDXYPYMNE and 2-acetylpyrrole (ACTLPYROLE), while for ALD was 2-methyl-butanal (M2BTAL), 3-methyl-butanal (M3BTAL) and 2-methyl-propanal (MPPAL). CAC contribution was explained by the presence of free fatty-acids, mainly by ETNOIC contribution. PYR contribution was principally influenced by MALTOL, and its derivatives, HX5MALTOL and 3-hydroxy-2,3-dihydro-maltol (HX3DH23MALTOL). VOCs from ALC, BNZ, EST, PHE and SUL were also identified in all stages, but only presented a considerable contribution (>1%) at some stages. ALC and BNZ are characterized by its considerable dimension, 16 and 13 VOCs, respectively. On the contrary, EST, PHE and SUL are characterized by its small dimension, lower than 10 VOCs. ALC presented a reasonable contribution in S1, S2 and S5, being principally explained by ETOL, and in minor extension, by 2-cyclohexenol (CHEX2E1OL). Also, 1-penten-3-ol (PT1E3OL) and 1-hexanol (HX1OL) in S1, and the sugar-alcohol erythritol (ERYTOL) in S5, presented a considerable contribution. The higher contribution of BNZ was observed in S5, being highly influenced by benzeneacetaldehyde (BENZACETAL), 3-methoxy-1,2-benzenediol (M3BNZDIOL) and 2-methyl-1,4-benzenediol (M2BNZ14DIOL). A substantial contribution of SUL was observed in S2, influenced by DMSULFI, while the contribution of EST in S5 was explained by ethyl acetate (EESTAA), vinylene carbonate (VYLESTCA) and 4,5-dimethyl vinylene carbonate (DM45VYLESTCA). The high contribution of PHE in S3, S4 and S5 was explicated by phloroglucinol (PHLOGLNOL), 4-amino-phenol (AMIPHEOL) and phenol (PHEOL). Although VOCs from BZF, ETH, HYD, NPH and TER were identified in all stages, its contribution were lower than 1% in all stages. In fact, these classes also presented small number of VOCs assigned, always lower than 5 VOCs.

There, the chemical classes highly related to NEBRs, such as FUR, BZF, PHE and PYR, and in minor extension, ALD, BNZ, KET and NIT, are responsible for 80% or more in S1 and S2, increasing to 90% in S3 and S4, and decreasing below 80% in S5. Recalling the existence of a sharp rise in temperature between S1 and S4 (40 to 120 °C), it is evident the occurrence of some thermal reactions in these stages, such as Maillard reaction, Streker degradation and caramelization. Nevertheless, some VOCs assigned in ALD, KET and NIT can be associated to others origins, being also formed in the raw material itself, or be products of enzymatic reactions and microbial activity that occurred in the raw material before being processed, or even during the storage of the SCH. VOCs from others chemical classes, namely ALC, CAC and EST, appears to be linked to action of enzymes (only in S1) and microorganisms due to its higher contribution in S1 and S5. On the other hand, VOCs from HYD and TER mainly found in S1, are probably from SC plant, being synthetized during several biochemical pathways. However, the origin of VOCs from IND, NPH and ETH are more difficult to explain. Due to the enormous diversity of VOCs within each chemical class, and also due to the complexity of their formation and origin, a chemometric analysis was used to obtain a more detailed view of each stage of SCH processing.

3.2. *Chemometric analysis based on the volatile profile throughout the sugarcane honey processing*

Chemometric analysis was performed to comprehend the formation and origin of VOCs in each stage, and mainly, to recognize the pathways involved during processing and storage of SCH, allowing the optimization and control of conditions for each stage in order to establish the

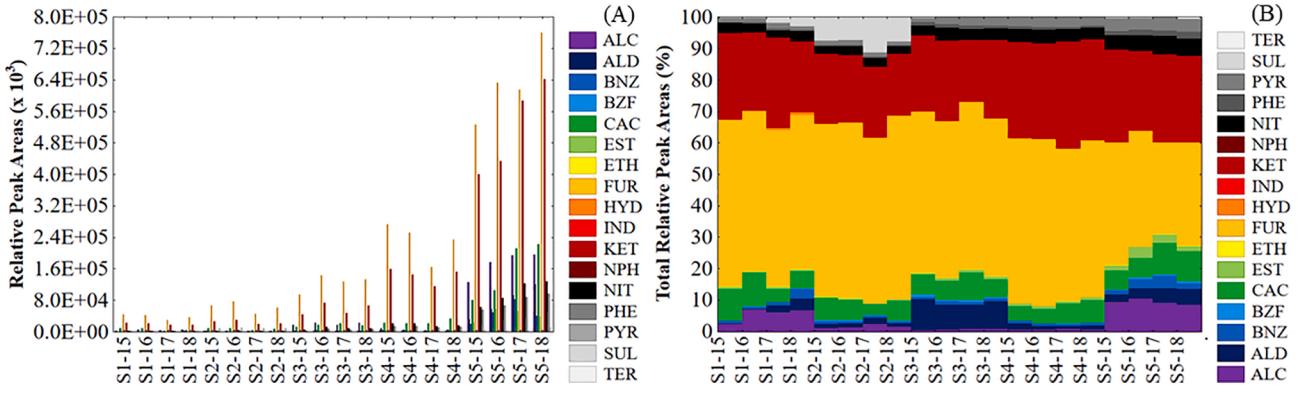

Fig. 2. Contribution, relative peak area (A) and % total relative peak area (B) values, of each classification group assigned according to chemical class for all stages.

typicality and authenticity of final product.

3.2.1. One-way ANOVA test

One-way ANOVA was performed to determine the VOCs with statistically significant differences based on its variance level throughout the SCH processing, namely between all stages, and S1-S2, S2-S3, S3-S4 and S4-S5 transitions. The data obtained from ANOVA was valuable to understand the formation pathways and origin of VOCs. The significance parameters, Probability (P) and Fischer (F) values, between all stages and for each transition are summarized in SM Table 7.

According with results from ANOVA test, all 187 VOCs presented statistically significant differences ($P < 0.05$) in RPA values between all stages (S1-S5), where 48 VOCs (25.7%) showed high differences (F values $\geq$ 100) between all five stages. Furthermore, 20 VOCs (10.7%) demonstrated very high significant differences (F values $\geq$ 200) throughout the SCH processing, namely DMSULFI, DHYPPAONE, 2,6-dimethyl-pyrazine (DM26PYZNE), ETOL, ACTYMFURALB, 2-ethyl-6-methyl-pyrazine (E6MPYZNE), octanal (OCTAL), HM5FURAL, HX3DH23MALTOL, FUREOL, MALTOL, 5-methyl-2(3H)-furanone (M5FURONE), M5FURAL, THDXYPYMNE, 1-(2-furanyl)-ethanone (FURYLONE), ACYLDHFURONE, C12PTDONE, pentanal (PTNAL), oxypurinol (OXYPUROL) and 4-cyclopentene-1,3-dione (CPT4E13DONE).

Likewise, the ANOVA results from each one of the four transitions between the stages during SCH processing (S1-S2, S2-S3, S3-S4 and S4-S5) showed that all 187 VOCs presented statistically significant differences in RPA values at least between one transition. Remarkably, 31 VOCs demonstrated significant differences throughout all transitions, namely DMSULFI, furan (FUR), 2-methyl-furan (M2FUR), 2-butanone (BT2ONE), M3BTAL, 5-butyl-dihydro-2(3H)-furanone (BDH2FURONE), m-cresol (MCREOL), 5-propyl-dihydro-2(3H)-furanone (PDH2FURONE), 2-methyl-dihydro-2(3H)-furanone (MDH2FURONE), M5FURONE, 1,3-dihydro-4-methyl-2H-imidazol-2-one (M4IMDZONE), furfuryl formate (FURYLFMTE), 2,2′-methylenebis[5-methyl-furan (MNEB5MFUR), CPT12DONE, 2,2-diethyl-3-methyl-oxazolidine (DEMOXZDNE), acrylamide (ACRYLMDE), 2,3-dimethyl-3-ppyrazolin-5-one (DM23PYZLONE), M2BNZ14DIOL, MALTOL, 2H-Pyran-2,6(3H)-Dione (PYR26DIONE), 1-(2-furanyl)-2-hydroxy-ethanone (H2FURYLONE), 1H-pyrrole-2-carboxaldehyde (PYRLE2AL), PHLOGLNOL, 2-furanpropionic acid (FURPPIONIC), DHYPPAONE, DM45VYLESTCA, 2-methoxy-4-vinyl-phenol (MXY2VYL4PHEOL), 4-pyridinol (PYRDINOL), HM5FURAL, FURYLETDIOL and DHYHYFURONE. Contrariwise, 36 VOCs presented statistically significant differences only for one specific transition. In S1-S2 transition, 76 VOCs presented significant differences, where 12 were specific from this transition, namely ethyl ether (EETHR), 3-pentanone (PT3ONE), methyl 2-ethylpentanoate (MESTPTA), 3-methyl-1-butanol (M3BT1OL), cis-2-pentenol (CPT1E2OL), 2-pentene (PT2ENE), 1-ethyl-1-methyl-cyclopentane (E1M1CYPTANE), 2-octanol (OCT2OL), trans-2-octenal (TOCT2EAL), 1-octen-3-ol (OCT3E1OL), trans-2-octenol (TOCTE2OL) and diethylene glycol monobutyl ether (DETNGOLBTHR). Despite 146 VOCs showed significant differences from S2 to S3, only hexane (HXANE), 2-heptanone (HPT2ONE), 1-pentanol (PT1OL), 2,5-dimethyl-pyrazine (DM25PYZNE), 3-ethyl-2-methyl-1,3-hexadiene (E3M2HX13DENE), 1,4-butanediol (BT14DIOL), 2-ethyl-phenol (E2PHEOL) and benzophenone (BENZPONE) were found to be specific for S2-S3 transition. For S3-S4 transition, 112 VOCs were significantly different in terms of RPA values, which mesitylene (MESTLNE) and naphthalene (NPHNE) presented only for this transition. Finally, in the last transition S4-S5, where SCH was stored during 6 months at room temperature, 149 VOCs demonstrated significant differences in RPA values. Among these, the following 16 VOCs were specific for this transition, ethyl formate (EESTFA), ethyl propanoate (EESTPA), 1-propanol (P1POL), nonomethyl succinate (METESTBA), dimethyl disulfide (DMDSFD), 2-methyl-1-propanol (M2PP1OL), 1-butanol (BT1OL), 2-methyl-1-butanol (M2BT1OL), 5-methyl-2-furanmethanethiol (M2FURTHOL), decanal (DECAL), 2,3-Dihydro-1,1,4,6-tetramethyl-1H-indene (DHT1146MIDNE), phenylmethyl acetate (PMESTAA), 2-phenylethyl acetate (PEESTAA), ERYTOL, octanoic acid (OCTOIC) and undecanoic acid (UNDECOIC).

Interestingly, the results from ANOVA test confirmed some information mentioned before (in Section 3.1.3). There, most of VOCs that showed significant differences between all transitions are related to NEBRs, such as M3BTAL, CPT12DONE, DHYPPAONE, HM5FURAL, M5FURONE and DHYHYFURONE. On the other hand, some specific VOCs from S1-S2 were originated from SC plant biochemistry, such as PT2ENE, CPT1E2OL, TOCTE2OL and PT3ONE, being probably degraded in S2. Furthermore, some specific VOCs from the transition S4-S5 are probable products of enzyme and microbial activity during SCH storage, such as EESTFA, EESTPA, P1POL and M2PP1OL.

3.2.2. Principal component analysis and partial least squares analysis

Principal Component Analysis (PCA) and Partial Least Squares (PLS) analysis were applied on RPA values of VOCs dataset in order to obtain the preview of differentiation/correlation structure based on the variance of samples from all stages of SCH processing between 2015 and 2018, without classification and with classification according to the stage, respectively. The information of PCA and PLS analysis are summarized in SM Table 8.

The loading results and VIP scores of PCA and PLS analysis for each variable (VOCs) are described in SM Table 9, while the loading results of all stages samples (PCA) and five stages centroids (PLS) are described in SM Table 10. The PCA and PLS scores results of all samples under analysis are described in SM Table 11. The PCA loadings line plot of all stages samples for PC1, PC2 and PC3 are showed in SM Fig. 2(A), (B) and (C), respectively. The PLS loadings line plot of five stages centroids for PLS1, PLS2 and PLS3 are showed in SM Fig. 2(D), (E) and (F), respectively. The PCA loading 3D plots of all stages samples and all variables for PC1, PC2 and PC3 are showed in Fig. 3(A) and (E), respectively. The PLS loading 3D plots of the five stages centroids and all variables for PLS1, PLS2 and PLS3 are showed in Fig. 3(B) and (F), respectively.

The PCA analysis based on PC1, PC2 and PC3 explained 72.99% of the total variance (TVA), being that the sum of all 14 components explained 96.88%. Despite the existence of some intra-variability between samples from S5 in PC1 and PC3, and S1 in PC2, the projection of all samples based on PC1, PC2 and PC3 loading results presented the formation of three well-defined groups according to SCH processing stage, namely the group formed by S1 samples, group formed by S5 samples, and a huge group formed by samples of intermediate stages, S2, S3 and S4. In PC1 projection (57.10% TVA), S5 samples demonstrated a high variance from the others samples stages. On the contrary, the projections of S1, S2, S3 and S4 samples in PC1 showed a low variance between stages, being observed a small but distinct difference between the projection of two group of samples, S1-S2 and S3-S4. Regarding the PC2 projection (8.70% TVA), S1 samples presented intra-variance among the four years of SCH production, mainly between 2015–2016 and 2017–2018. However, S1 samples also demonstrated high variance from S2, S3 and S4 samples, and in minor extension, from S5 samples. Also, the S3 and S4 samples presented a considerable variance from S1, S2 and S5 samples. According the PC3 projection (7.20% TVA) was observed a small variance between S1, S2, S3 and S4 samples. Nevertheless, a huge intra-variance was presented among the samples from S5. The projections of S5 in PC1 and PC3 indicate that the storage conditions should be more strictly controlled. Additionally, the period of time until the product sale could be a factor influencing the volatile profile of SCH. On the other hand, the stages associated to thermal processing (S2, S3 and S4) presented low intra-variance among the samples from the four years under study.

A PLS analysis was applied to confirm the variance between samples when classified according to stage of SCH processing, being classified as: centroid-S1 (CS1), centroid-S2 (CS2), centroid-S3 (CS3), centroid-S4 (CS4) and centroid-S5 (CS5). The three main partial least squares (PLS1, PLS2 and PLS3) explained 78.16% of TVA, where the sum of all 20 components explained 99.96%. As expected, an important variance

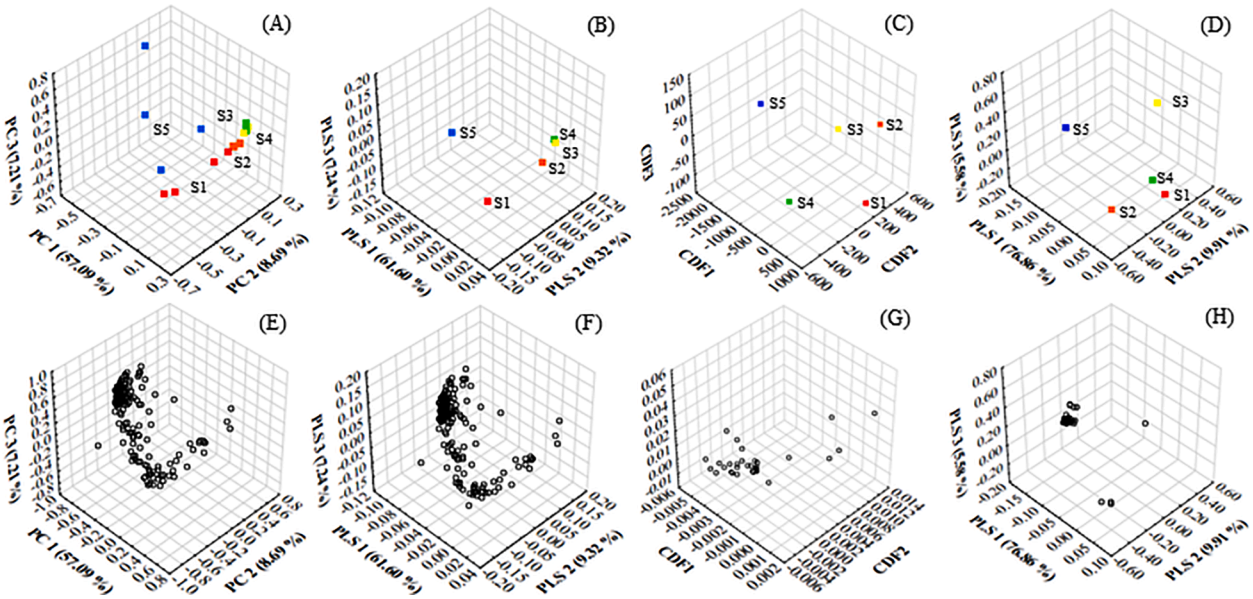

Fig. 3. PCA loading 3D plot of all stages samples (A) and the selected 187 VOCs (E) for the three main components. The PLS loading 3D plot of all stages centroids (B) and the selected 187 VOCs (F) for the three main components. The LDA loading 3D plot of all stages centroids (C) and the 35 most predictive VOCs (G) for the three main components. The PLS loading 3D plot of all stages centroids (D) and the 35 most predictive VOCs (H) for the three main components.

was observed in projection of three main components between the CS1, CS5, and group formed by CS2, CS3 and CS4, being observed a slight variance between CS2 and CS3-CS4. In PLS1 projection (61.60% TVA), the CS5 presented a high variance from the others centroids. Even though in minor extension, the CS1, CS2, CS3 and C-S4 also demonstrated a good variance in PLS1 projection, principally between CS1-CS2 and CS3-CS4. In PLS2 (9.30% TVA), CS1, CS2, CS5, and CS3-CS4 centroids exhibited a substantial variance from the others, where the higher variance was verified for CS1. As PLS1, in PLS3 (7.20% TVA), the higher variance was also reached between CS5 and the others centroids.

Although the PLS model was constructed based on all 187 VOCs, each one influenced differently the projection of centroids, being possible to observe the contribution of each VOC for the projection of a centroid associated with a specific stage of SCH processing. On the main PLS projection (PLS1), the most of VOCs influenced the CS5, where was highly influenced by 115 VOCs (61.50%), belonging a wide variety of chemical classes, which some can be highlighted due to their potential source or chemical pathway. Although some VOCs belong to chemical classes related to activity of microorganisms, namely ALC (i.e. ETOL), CACD (i.e. ETNOIC) and EST (i.e. PMESTAA and PEESTAA), most of VOCs belong to chemical classes associated a NEBRs, such as KET (i.e. 3-hydroxy-2-butanone (HXY3BT2ONE), HXY1PP2ONE and DHYPPAONE), PYR (i.e. MALTOL, HX3DH23MALTOL and HX5MALTOL), NIT (DM26PYZNE and E6MPYZNE), and FUR (i.e. FURAL, HM5FURAL, M5FURONE, DHYHYFURONE, H2FURYLONE and FUR2OL). The influence demonstrated by these VOCs in S5 indicate that is possible the occurrence of NEBRs during the storage period, at least in the first months. Interestingly, the projections of CS1 and CS2, and in minor extension, CS3 and CS4, were strongly influenced by 40 VOCs (21.39%), namely ALC (i.e. 2-methyl-3-buten-2-ol (M3BT2OL), 1-penten-3-ol (PT1E3OL), M3BT1OL, PT1OL, CPT1E2OL, 2-heptanol (HPT2OL), HX1OL, TOCTE2OL, 1-heptanol (HPT1OL), 1-octanol (OCT1OL), OCT2OL and BT14DIOL), KET (i.e. PT3ONE, 1-penten-3-one (PT1E3ONE), HPT2ONE, 3-octanone (OCT3ONE) and 2-nonen-4-one (NON2ONE)), ALD (i.e. PTNAL, hexanal (HXAL), heptanal (HPTAL), OCTAL, *cis*-2-heptanal (CH2PTAL), TOCT2EAL and (E,E)-2,4-heptadienal (TTHPT24DAL)) and HYD (i.e. 1,4-pentadiene (PT14DIENE), PT2ENE, E1M1CYPTANE and E3M2HX13DENE). There, VOCs are probably formed in SC plant, or later, by action of enzymes and microorganisms in SC raw material, or even in initial steps of NEBRs (i.e. Maillard reaction).

3.2.3. *Linear discriminant analysis and hierarchical clustering analysis*

Linear discriminant analysis (LDA) was applied as supervised pattern recognition method in order to obtain classification rules for the group assignment (S1, S2, S3, S4 and S5) of all samples under analysis based only in the most predictive VOCs. A matrix reduction procedure was used due to the complexity of applying the LDA to a large number of variables. The LDA information of the selected 37 VOCs based on the VIP scores are summarized in SM Table 14. However, the procedure based on the VIP scores presented poor results on PLS and HCA analysis (showed in SM Fig. 5), being ignored for further analysis. The CDF coefficients and highest probability classification results of all samples are summarized in SM Table 12. The LDA line plots of all stages classified according to CDF1, CDF2 and CDF3 are exposed in SM Fig. 3 (A), (B) and (C), respectively. The LDA line plot of most predictive VOCs for CDF1, CDF2 and CDF3 are presented in SM Fig. 3(D), (E) and (F), respectively. The CDF coefficients 3D plots of the five stage centroids and most predictive VOCs for CDF1, CDF2 and CDF3 are presented in Fig. 3 (C) and (G), respectively. The LDA information and canonical discriminant function (CDF) coefficients of the most predictive VOCs based on F-Vale from one-way ANOVA test are summarized in Table 1.

All samples under analysis were classified at 100% correct rate, being clustered according the five stages of SCH processing. Only two VOCs were removed from LDA analysis through 89 steps of the backward selection method ($p < 0.05$), PTNAL and CPT4E13DONE. Therefore, LDA analysis were only based on the 35 most predictive VOCs, namely DMSULFI, DHYPPAONE, DM26PYZNE, ETOL, ACTYMFURALB, E6MPYZNE, OCTAL, HM5FURAL, HX3DH23MALTOL, FUREOL, MALTOL, M5FURONE, M5FURAL, THDXYPYMNE, FURYLONE, ACYLDHFURONE, CPT12DONE, OXYPUROL, 4-(1-methylpropyl)-phenol (MPPYLPHEOL), OCTOIC, MDH2FURONE, 3-methyl-2(5H)-furanone (M3FURONE), 1,4:3,6-dianhydro-.alpha.-d-glucopyranose (GLUPYROSE), 2-propenal (PPENAL), FURAL, HX5MALTOL, PYRDINOL, FURYLETDIOL, DHYHYFURONE, ACTLPYROLE, 3-methyl-2,4(3H,5H)-furandione (M3FURDIONE), ACRYLMDE, PYR26DIONE, NON2ONE and 3-methyl-dihydro-2(3H)-furanone (M3DHFURONE). Remarkaly, >80% of 35 most predictive VOCs are related to thermal degradation, while the remaining VOCs are mostly associated with enzyme and microbial activity.

Table 1
Results of variables from Linear Discriminant Analysis (LDA) after matrix reduction method to 20% of original dimension according with higher Fisher values obtained from One-way ANOVA test based on the relative peak areas of the identified VOCs in samples from SCH processing stages during 2015–2018 production years.

Volatile Organic Compounds	Abbreviations	ANOVA	LDA					PLS				
		F[1]	W[2]	F[3]	CDF[4]			Loading Value			VIP[5]	
					1	2	3	1	2	3	Importance	Power (x 100)
Dimethyl Sulfide	DMSULFI	562.68	5.05E-05	1.04E + 05	0.00101	0.01304	0.02882	0.041	−0.480	−0.059	3.0	22.77
1,3-Dihydroxy-2-Propanone	DHYPPAONE	549.57	2.07E-03	2.53E + 03	−0.00512	−0.00305	−0.00098	−0.179	0.000	−0.040	31	8.01
2,6-Dimethyl-Pyrazine	DM26PYZNE	523.62	1.71E-03	3.06E + 03	−0.00494	0.00047	0.01127	−0.171	−0.002	0.153	13	16.50
Ethanol	ETOL	409.24	2.27E-04	2.32E + 04	−0.00445	0.00201	−0.00198	−0.176	−0.061	−0.014	34	7.84
5-Acetoxymethyl-2-Furfural B	ACTYMFURALB	395.90	3.17E-04	1.66E + 04	−0.00436	−0.00223	−0.00144	−0.178	−0.005	−0.044	12	16.59
2-Ethyl-6-Methyl-Pyrazine	E6MPYZNE	369.28	1.10E-03	4.78E + 03	−0.00413	0.00048	0.00998	−0.171	−0.004	0.162	19	13.65
Octanal	OCTAL	343.03	1.33E-02	3.89E + 02	0.00156	0.00337	0.05184	0.069	−0.111	0.594	5	21.42
5-(Hydroxymethyl)-2-Furfural	HM5FURAL	338.26	5.39E-04	9.73E + 03	−0.00380	−0.00515	0.00578	−0.167	0.015	−0.023	10	18.77
3-Hydroxy-2,3-Dihydro-Maltol	HX3DH23MALTOL	318.36	5.83E-03	8.95E + 02	−0.00389	−0.00252	−0.00060	−0.178	0.004	−0.036	21	10.74
Furaneol	FUREOL	315.94	9.31E-02	5.11E + 01	−0.00379	−0.00412	0.00044	−0.170	0.041	−0.031	15	16.33
Maltol	MALTOL	261.99	5.44E-03	9.59E + 02	−0.00358	0.00002	−0.00057	−0.179	−0.039	−0.020	35	6.60
5-Methyl-2(3H)-Furanone	M5FURONE	251.27	9.07E-02	5.26E + 01	−0.00134	−0.00055	0.00002	−0.161	−0.005	−0.017	4	21.87
5-Methyl-Furfural	M5FURAL	248.78	1.28E-03	4.10E + 03	−0.00348	−0.00115	0.00089	−0.178	−0.018	−0.008	14	16.49
2,4,6-Trihydroxypyrimidine	THDXYPYMNE	230.84	3.30E-03	1.59E + 03	−0.00330	−0.00242	−0.00078	−0.176	0.007	−0.046	18	14.29
1-(2-Furanyl)-Ethanone	FURYLONE	225.90	3.70E-04	1.42E + 04	−0.00320	−0.00302	0.00732	−0.173	0.043	0.102	6	20.78
5-Acetyl-Dihydro-2(3H)-Furanone	ACYLDHFURONE	224.75	2.12E-03	2.47E + 03	−0.00325	−0.00265	0.00051	−0.177	0.018	−0.017	16	16.25
1,2-Cyclopentanedione	CPT12DONE	220.79	1.43E-03	3.66E + 03	−0.00327	−0.00155	0.00130	−0.179	−0.002	0.005	27	9.24
Pentanal	PTNAL	213.44	Removed from analysis.									
Oxypurinol	OXYPUROL	204.15	1.27E-03	4.12E + 03	−0.00316	0.00008	−0.00142	−0.179	−0.036	−0.026	28	9.22
4-Cyclopentene-1,3-dione	CPT4E13DONE	200.16	Removed from analysis.									
4-(1-Methylpropyl)-Phenol	MPPYLPHEOL	187.99	3.84E-03	1.36E + 03	0.00097	0.00655	0.01898	0.062	−0.455	−0.040	2	24.56
Octanoic Acid	OCTOIC	183.47	8.26E-02	5.83E + 01	−0.00298	0.00132	−0.00107	−0.169	−0.055	−0.010	11	16.75
2-Methyl-Dihydro-2(3H)-Furanone	MDH2FURONE	183.31	6.09E-02	8.09E + 01	−0.00299	0.00097	0.00085	−0.176	−0.049	0.028	25	9.63
3-Methyl-2(5H)-Furanone	M3FURONE	177.33	3.00E-02	1.70E + 02	−0.00295	0.00007	−0.00015	−0.178	−0.030	0.004	32	7.99
1,4:3,6-Dianhydro-.alpha.-d-Glucopyranose	GLUPYROSE	146.81	6.26E-04	8.38E + 03	−0.00268	0.00052	−0.00004	−0.175	−0.049	0.000	23	10.34
2-Propenal	PPENAL	139.12	1.66E-03	3.16E + 03	−0.00261	0.00041	0.00091	−0.165	−0.021	0.029	9	19.66
Furfural	FURAL	137.75	9.76E-04	5.37E + 03	−0.00239	−0.00366	0.00665	−0.168	0.066	0.103	7	20.36
5-Hydroxy-Maltol	HX5MALTOL	136.53	9.92E-02	4.77E + 01	−0.00258	−0.00048	−0.00035	−0.178	−0.023	−0.015	29	9.17
4-Pyridinol	PYRDINOL	135.63	7.83E-04	6.70E + 03	−0.00258	0.00016	−0.00014	−0.178	−0.042	−0.007	30	8.28
1-(2-Furanyl)-1,2-Ethanediol	FURYLETDIOL	134.76	2.51E-04	2.09E + 04	−0.00257	−0.00042	−0.00080	−0.177	−0.016	−0.017	8	19.82
4-Hydroxy-Dihydro-2(3H)-Furanone	DHYHYFURONE	132.15	1.35E-03	3.88E + 03	−0.00173	0.00409	0.00327	−0.178	−0.040	−0.018	33	7.92
2-Acetylpyrrole	ACTLPYROLE	129.05	2.03E-04	2.58E + 04	−0.00251	−0.00010	0.00174	−0.177	−0.023	0.044	22	10.50
3-Methyl-2,4(3H,5H)-Furandione	M3FURDIONE	128.42	3.24E-02	1.57E + 02	−0.00251	0.00010	−0.00005	−0.178	−0.038	−0.002	26	9.48
Acrylamide	ACRYLMDE	126.86	2.53E-04	2.07E + 04	−0.00249	0.00006	0.00003	−0.176	−0.044	−0.013	24	10.17
2H-Pyran-2,6(3H)-Dione	PYR26DIONE	121.86	2.84E-04	1.85E + 04	−0.00244	−0.00005	−0.00051	−0.176	−0.033	−0.017	20	11.46
2-Nonen-4-one	NON2ONE	121.21	5.71E-04	9.19E + 03	0.00078	0.00526	0.01524	0.060	−0.453	−0.024	1	24.69
3-Methyl-Dihydro-2(3H)-Furanone	M3DHFURONE	121.00	3.43E-04	1.53E + 04	−0.00244	−0.00005	0.00019	−0.175	−0.027	0.003	17	14.57

[1] F - Fischer value from One-way ANOVA test.
[2] W - Wilks value from Linear Discriminant Analysis.
[3] F - Fischer value from Linear Discriminant Analysis.
[4] CDF - Canonical Discriminant Function Coefficients.

The LDA results demonstrated a high level of discrimination along the three CDFs between the samples from the five stages. In CDF 1, a notable discrimination was obtained between the samples from S5 and others stages. For CDF 2, the higher discrimination was observed between samples of S4 and others stages. Also, in CDF2, a reasonable discrimination was observed between S1, S2, S3 and S5. For CDF3, a high discrimination level was observed in samples of S1 from the others samples, being also verified a considerable discrimination between others stages. LDA results proved that the is possible discriminate and classify correctly all samples from each one of the five stages of SCH processing based on the RPA values of the 35 most predictive VOCs, corresponding to 17.1% of the original matrix of 187 VOCs.

3.2.4. *Partial least squares and hierarchical clustering analysis*

An additional PLS analysis based only on the 35 most predictive VOCs were done to confirm the differentiation/correlation structure between all stages of SCH processing. The PLS information are summarized in SM Table 13. The loading results and VIP scores from PLS analysis of all 35 VOCs are summarized in Table 1. The PLS loading results of stages centroids and the scores results of all samples under analysis are described in SM Table 12. The PLS loadings line plots of all stages classified according to PLS1, PLS2 and PLS3 are showed in SM Fig. 4(A), (B) and (C), respectively. The PLS loadings line plot of the 35 most predictive VOCs for PLS1, PLS2 and PLS3 are showed in SM Fig. 4 (D), (E) and (F), respectively. The PLS loading 3D plots of the five stages centroids and 35 most predictive VOCs for PLS1, PLS2 and PLS3 are showed in Fig. 3(D) and (H), respectively.

The PLS analysis based on PLS1, PLS2 and PLS3 explained 92.4% of TVA, where the sum of all 16 components explained 99.9%. There, a high inter-variance between was observed between all stages centroids, even between CS2, CS3 and CS4. Expectably, in PLS1 (76.9%) the higher variance was verified between CS5 and others stages centroids, being also verified a considerable inter-variance between two groups of stages CS1-CS2 and CS3-CS4. Regarding the PLS2 projection (9.9%), a substantial variance was observed between CS2 and other stages centroids. Finally, in PLS3 projection (5.6%), a high variance was verified between S3 and other centroids. The projection of three main component from PLS based on the 35 most predictive VOCs presented a considerably higher differentiation between all stages centroid when compared to similar projection of the PLS performed with all 187 VOCs. In line with the previous results, through the analysis of the 35 most predictive VOCs in the projection of main component (PLS 1), it is possible to verify the influence of some VOCs with one or two specific stages of the processing of the SCH. There, close to 83% of most predictive VOCs influenced the projection of S5, where mainly are related to NEBRs, such as DHYPPAONE, DM26PYZNE, FURAL, HM5FURAL, FUREOL or MALTOL. Also, ETOL, a VOC that influenced highly the projection of S5, is a well-known product from alcoholic fermentation. On the contrary, only four VOCs, DMSULFI, OCTAL, MPPYLPHEOL and NON2ONE, influenced the projection of remaining stages. Despite this specific influence, all 35 most predictive VOCs can be considered as potential markers for control of SCH processing, which should be developed in further studies to achieve its quantification.

HCA was performed based on the RPA values of previously selected 35 VOCs in order to determine the linkage Euclidean distances between all samples and complete an appropriate measure of distance and linkage criterion between the five stages of SCH processing. The HCA dendrogram is presented in Fig. 4.

As expected, the higher distance was achieved between the S5 and other stages, where the linkage level of samples decreases as follows: S5 > S4 > S3 > S2 > S1. The HCA results showed a perfect grouping of all samples according its stage of SCH processing. Moreover, low distances were obtained for samples of similar stage throughout the four years under study, demonstrating the high consistence of obtained results based on the most predictive VOCs. Thus, the results from second PLS and HCA confirm that is possible the establishment of typicality and authenticity of SCH through rigorous procedures and strict control of all stages during its traditional processing and storage based on the analysis of the 35 most predictive VOCs.

3.3. *Formation pathways model of volatile profile throughout the SCH making process*

Comprehensively, the origin and formation of VOCs from SCH is not simple to explain, where a wide and complex network of interconnecting chemical pathways can be involved throughout all stages. Nevertheless,

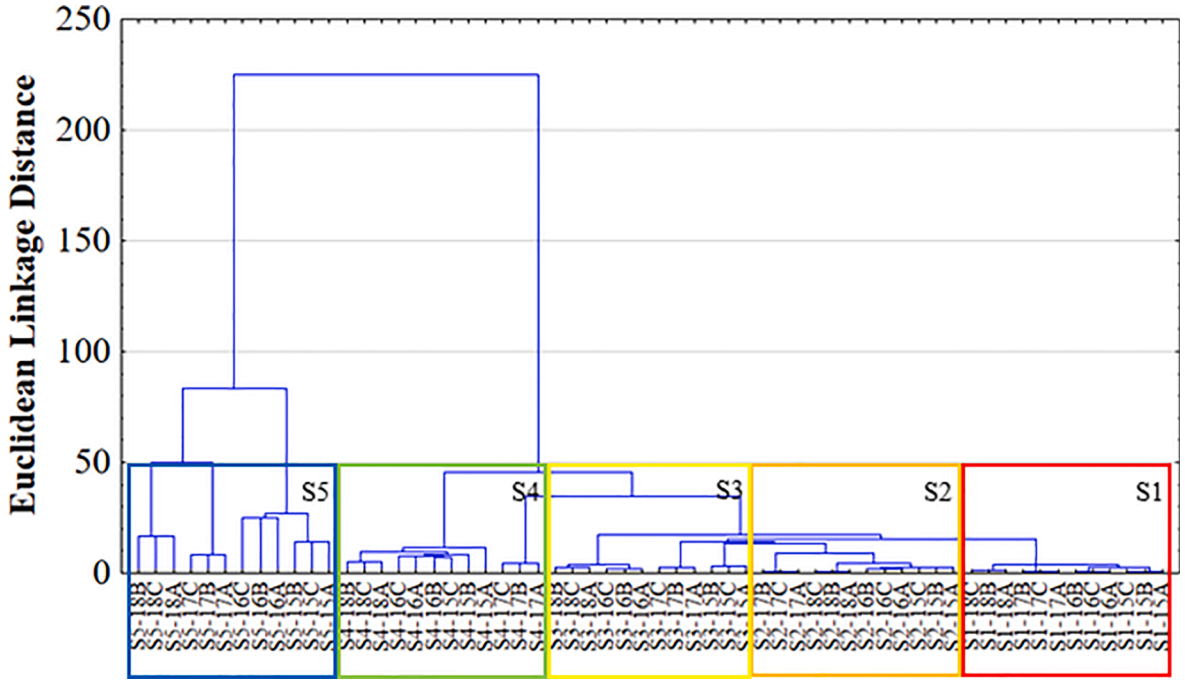

Fig. 4. HCA dendrogram based on Euclidean linkage distances for all replicates (A, B and C) from all stages.

based on the results previously described, and supported by the available information from the scientific literature, is possible to propose a preliminary model of VOCs formation pathways during all stages of SCH processing, being summarized in Fig. 5.

The proposed model of formation pathways was constructed according the conditions of processing at each stage (i.e. temperature, water content, atmosphere exposure) and the formerly recognized components of SC raw material (i.e. polyphenols, lipids, L-ascorbic acid, sugars and amino acids), corresponding the main reactions or pathways that probably occur at each stage, and consequently, the chemical class of its products.

Firstly, some VOCs from BNZ, TER and HYD were found in higher quantities in S1 and S2, such as MESTLNE, p-cymene (PCYMNE) and PT2ENE, being VOCs linked to SC plant biochemistry, where play a key role in plant-environment interactions, abiotic stress response and microbial pathogens defense (Bergman & Phillips, 2021; Eyong, Kuete, & Efferth, 2013; Tian et al., 2019). Likewise, a wide diversity of short-chain VOCs from ALC, ALD, EST and KET found in S1 and S2 were also found in various plant tissues, being formed *in vivo* by several enzymes (Dudareva, Klempien, Muhlemann, & Kaplan, 2013). In fact, these VOCs are probably formed during the crushing and pressing of SC stalks in S1, where the activity of enzymes is exponentially increased due to the disruption of plant tissues (Xu, Luo, Charles, Rolland, & Roussel, 2017). Lipoxygenase (LOX) and peroxidase (POX) can oxidize lipids (free fatty-acids) to form several VOCs from ALD and KET (Suzuki et al., 2010; Zhou, Sun, Li, Zhu, & Tu, 2019). Polyphenol oxidase (PPO) and POX oxide the polyphenols into quinones, which in later reactions with amino acids can generated ALD-VOCs (Rizzi, 2008). Also, ascorbic acid oxidase (AAO), a copper-containing enzyme, catalyze the oxidation of vitamin C to originate ALD-VOCs (Raseetha, Oey, Burritt, Heenan, & Hamid, 2013). Alcohol dehydrogenase (ADH) and alcohol acyltransferase (AAT) can react with previously formed aldehydes to produce short-chain ALC-VOCs (Dudareva et al., 2013). Moreover, several VOCs from ALC, ALD, BNZ, CAC, EST, HYD, KET and SUL identified in S1 and S2, can also be naturally formed by bacteria, fungi or yeast during the period of harvest and transportation of stalks to the factory, the storage before entering into the processing line and even in S1 and S2 processing (Thompson, 2009; Wang et al., 2016). Here, we can highlight the microbial formation of three VOCs that were classified as the main contributors to volatile profile of S1 and S2, namely ETNOIC, DMSULFI and ETOL. ETNOIC can be formed by oxidation of sugars and alcohols during fermentation process by acetic acid bacteria group (Sengun & Karabiyikli, 2011), DMSULFI can be produced by yeast-mediated mechanism during alcoholic fermentation (Deed et al., 2019), and ETOL can be easily produced by *Saccharomyces cerevisiae* in juice and syrups from SC (Kanakaraju et al., 2020). Additionally, in S1, and principally in S2, some NEBRs are initiated. Several short-chain VOCs from ALD and KET can be generated by lipid oxidation, mainly due to high temperature (>80 °C) used in S2 (Clarke, O'Sullivan, Kerry, & Kilcawley, 2020). Also, the temperatures used in S2 can promote the thermal degradation of L-ascorbic acid by reactions with some amino acids, where are formed VOCs from ALD, FUR and NIT (Tan & Yu, 2012). In addition, in S1 and S2 appear to occur the initial stages of Maillard Reactions between amino acids and sugars, where are formed a wide diversity of VOCs, mainly belong to ALD, KET, FUR and NIT. Summarizing the contribution of most chemical classes in S1 and S2, these can arise from two different origins, raw material and SCH processing. ALC-VOCs, such as CPT1E2OL and TOCTE2OL, were probably generated in SC plant tissues, while PT1OL, HX1OL, HPT1OL and OCT1OL are generated by thermal reactions (Hammerbacher, Coutinho, & Gershenzon, 2019; Maire, Rega, Cuvelier, Soto, & Giampaoli, 2013). Similary, VOCs from ALD and KET groups can be commonly found in various plant tissues, such as CH2PTAL and TOCT2EAL for ALD, and PT3ONE and OCT3ONE for KET (Hammerbacher et al., 2019). However, its probable main route of formation occurs during the all stages of thermal processing by a wide diversity NEBRs. For example, KET-VOCs, such as DHYPPAONE, BT23DONE and CPT12DONE, and ALD-VOCs such as MPPAL, M2BTAL and M2BTAL, can be generated during any of the follow NEBRs, namely lipid oxidation, L-ascorbic acid degradation, Maillard reactions, caramelization and melanoidins degradation (Cerny & Herrmann, 2010).

In S3 and S4, similar reactions to S2 occurred by thermal processing, where the caramelization process and melanoidins degradation can be added due to high temperatures used (up to 100 °C), promoting the formation of a large number of FUR-VOCs, where some are main contributors in S2, S3 and S4, being well-established markers of Maillard Reactions and caramelization, such as HM5FURAL, FURAL, HY2DHFURONE, HM5FURONE, FUR3OL (Cerny & Herrmann, 2010;

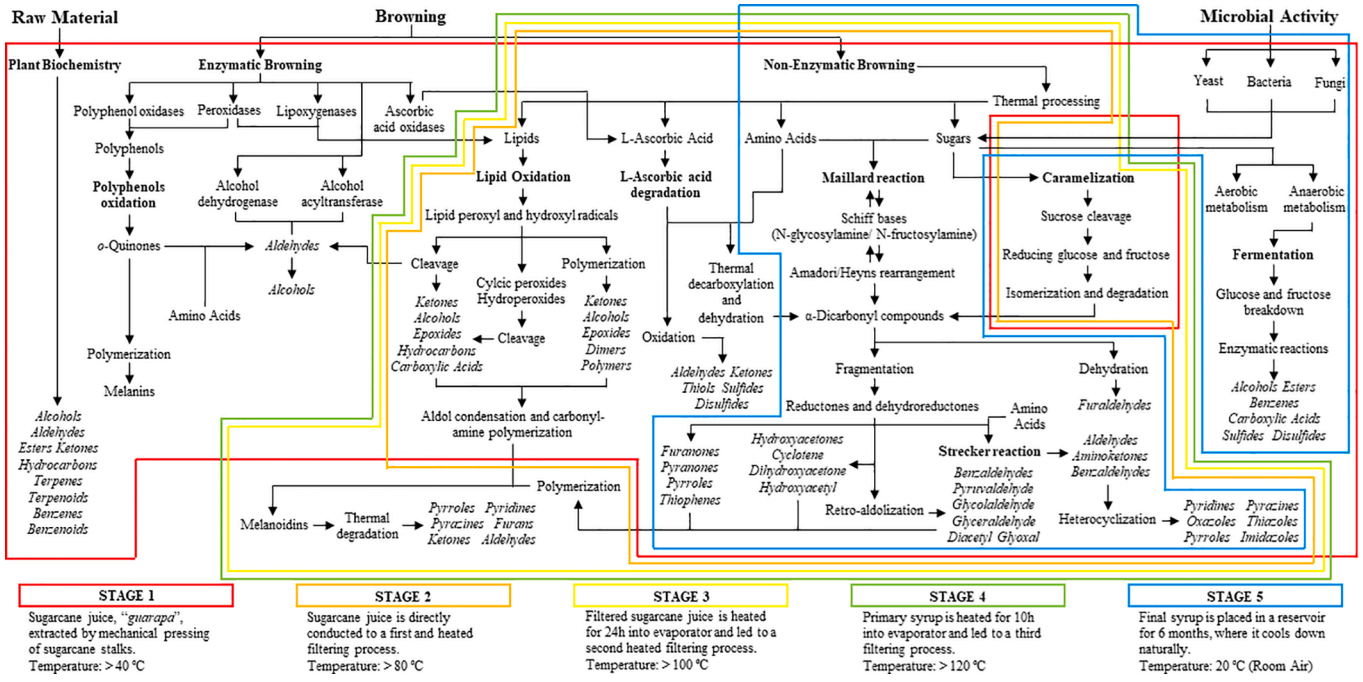

Fig. 5. Schematic diagram of VOCs formation pathways according to the conditions of processing at each stage.

Santos-Zea et al., 2016). Also, in S2, S3 and S4, a wide variety VOCs from ALD, KET, BZF, BNZ, NIT, PYR and PHE are formed. For example, NIT-VOCs, such as DM25PYZNE and ACTLPYROLE, are described as final products from Maillard reactions, Strecker reaction, caramelization and melanoidins degradation (Cerny & Herrmann, 2010; Hammerbacher et al., 2019). Likewise, PYR-VOCs, such as MALTOL and its derivatives, HX3DH23MALTOL and HX5MALTOL, are well-known products of last stages of Maillard reactions and caramelization that occurs during thermal degradation of sugary products (Parker, 2015). In addition, BNZ-VOCs, such as benzaldehyde (BENZAL) and BENZACETAL, are common products of Maillard reactions, principally during the Strecker degradation (Adamiec, Rössner, Velíšek, Cejpek, & Šavel, 2001; Cui et al., 2017). Although BZF-VOCs can be found in natural sources (i.e. plants, marine, fungus and bacteria), the two VOCs identified in all stages of SCH processing, namely 2-methyl-benzofuran (M2BNZFUR) and 2,3-dihydro-benzofuran (DHBNZFUR), are commonly formed as products of the Maillard reactions (Heravi, Zadsirjan, Hamidi, & Tabar Amiri, 2017; Yu, Zhao, Hu, Zeng, & Bai, 2012).

Finally, in S5, certainly the most important stage for typicality of SCH, the thermal reactions continue to occur, at least for the first few weeks in storage, and from there, it is possible to verify a considerable microbiological activity, probably due to the action of yeasts associated with alcoholic fermentation, leading to formation of VOCs from ALC, ALD, CAC, BNZ, EST and SUL. A substantial contribution of EST-VOCs, such as EESTFA and EESTPA, was observed in S5, where were probably formed by fermentation during SCH storage (Sumby, Grbin, & Jiranek, 2010). Also, ALC group demonstrated a high contribution in S5, being highly influenced by ETOL, and in minor extension, also by P1POL and M2PP1OL, where were apparently formed by action of microorganism during the SCH storage (Kanakaraju et al., 2020). While the higher contribution of BNZ-VOCs in S5 indicated its presumable microorganisms formation. For example, benzoic acid (BNZOIC) can be produced by microorganisms in food, (Joye, 2018). Moreover, some BNZ-VOCs can arise from degradation/conversion of BNZOIC, namely toluene (TOLNE) and benzenemethanol (BENZMTOL) (Bocharova, Reshta, & Eshtokin, 2017). Furthermore, some FUR-VOCs, such as FURYLFMTE, furfuryl acetate (FURYLACTE) and M2FURTHOL, had high RPA values only in the last stage, being probably also formed during the SCH storage by fermentation.

4. Conclusions

This study presents, for the first time, the monitoring of volatile profile throughout all stages (S1, S2, S3, S4 and S5) of SCH processing during four years (2015, 2016, 2017 and 2018) by a certified producer, in order to characterize the volatile profile developed in each stage, and consequently, establish the typicality and authenticity of SCH.

Based on obtained results, a preliminary model of VOCs formation pathways throughout the SCH processing is proposed, and consequently, contributed for the following conclusions. The volatile profile of S1 was influenced by EBRs, principally by enzymatic activity on the SC juice, and later, by NEBRs based on thermal degradation of L-ascorbic acid, lipid oxidation, Maillard reactions and Strecker degradation. In S2, S3 and S4, the thermal degradation reactions similar to S1 occurred at higher extension, where in S3 and S4 also occurred the caramelization and melanoidins degradation due to high temperatures used in these stages. Finally, in S5, the previously described thermal reactions continue to occur in first few weeks, being followed by microbial activity on the sugary components of SCH.

Thus, we conclude that is possible to establish a volatile profile for each stage of traditional SCH processing. Nevertheless, the volatile profile of SCH are strongly influenced by S5, where a strict and rigorous control is recommended in order to maintain the typicality and authenticity of SCH on the market. In this context, the 35 most predictive VOCs can be a valuable markers of SCH processing, being important its further quantification. Interestingly, the microbial activity that occurs naturally during the storage of SCH can give rise to new and differentiated products. For example, SCH can be marketed under controlled aging, following the example of liqueur wines, such as Madeira wine. Contrariwise, regarding the optimization of SCH processing, the S3 and S4 can be combined in a single stage, due to its low level of differentiation. In conclusion, these obtained results are a promising and useful data in order to define the typicality and authenticity of SCH, promoting its European certification and, consequently, avoiding potential frauds in the market. Additionally, the data obtained from this study about the VOCs formation can be valuable in order to comprehend the role and importance of BRs on food product, creating a preliminary database to support further studies in Foodomics domain.

CRediT authorship contribution statement

Pedro Silva: Conceptualization, Investigation, Methodology, Visualization, Writing – original draft. **Jorge Freitas:** Conceptualization, Methodology, Investigation, Writing – review & editing. **Fernando M. Nunes:** Conceptualization, Funding acquisition, Supervision, Methodology, Writing – review & editing. **José S. Câmara:** Conceptualization, Funding acquisition, Project administration, Supervision, Methodology, Writing – review & editing.

Declaration of Competing Interest

The authors declare that they have no known competing financial interests or personal relationships that could have appeared to influence the work reported in this paper.

Acknowledgements

The authors acknowledge the *Fábrica Mel-de-Cana Ribeiro Sêco de V. Melim, Lda, (*FMCRS*)*, Funchal, Portugal, and the *Agência Regional para o Desenvolvimento da Investigação, Tecnologia e Inovação (*ARDITI*)* through the support granted under the M1420 Project - 09-5369-FSE-000001 - PhD Scholarship in companies for PhD grant of the author Pedro Silva. This work was supported by FCT-Fundação para a Ciência e a Tecnologia through the CQM Base Fund - UIDB/00674/2020, and Programmatic Fund - UIDP/00674/2020, and by ARDITI-Agência Regional para o Desenvolvimento da Investigação Tecnologia e Inovação, through the project M1420-01-0145-FEDER-000005 - Centro de Química da Madeira - CQM+ (Madeira 14-20 Program). The authors also acknowledge the financial support from Fundação para a Ciência e Tecnologia and Madeira 14-2020 program to the Portuguese Mass Spectrometry Network (PROEQUIPRAM, M14-20M1420-01-0145-FEDER-000008).

Appendix A. Supplementary data

Supplementary data to this article can be found online at https://doi.org/10.1016/j.foodchem.2021.130457.

References

Abe, E., Nakatani, Y., Yamanishi, T., & Muraki, S. (1978). Studies on the“ sugary flavor” of raw cane sugar. I. Proceedings of the Japan Academy. Ser. B: Physical and Biological Sciences, 54(9), 542–547. DOI:10.2183/pjab.54.542.

Adamiec, J., Rössner, J., Velíšek, J., Cejpek, K., & Šavel, J. (2001). Minor Strecker degradation products of phenylalanine and phenylglycine. *European Food Research and Technology, 212*(2), 135–140. https://doi.org/10.1007/s002170000234.

Asikin, Y., Hirose, N., Tamaki, H., Ito, S., Oku, H., & Wada, K. (2016). Effects of different drying-solidification processes on physical properties, volatile fraction, and antioxidant activity of non-centrifugal cane brown sugar. *LWT - Food Science and Technology, 66*, 340–347. https://doi.org/10.1016/j.lwt.2015.10.039.

Asikin, Y., Kamiya, A., Mizu, M., Takara, K., Tamaki, H., & Wada, K. (2014). Changes in the physicochemical characteristics, including flavour components and Maillard reaction products, of non-centrifugal cane brown sugar during storage. *Food Chemistry, 149*, 170–177. https://doi.org/10.1016/j.foodchem.2013.10.089.

Asikin, Y., Wada, K., Imai, Y., Kawamoto, Y., Mizu, M., Mutsuura, M., & Takahashi, M. (2018). Compositions, taste characteristics, volatile profiles, and antioxidant activities of sweet sorghum (Sorghum bicolor L.) and sugarcane (Saccharum

officinarum L.) syrups. *Journal of Food Measurement and Characterization, 12*(2), 884–891. https://doi.org/10.1007/s11694-017-9703-2.
Bergman, M. E., & Phillips, M. A. (2021). Structural diversity and biosynthesis of plant derived p-menthane monoterpenes. *Phytochemistry Reviews, 20*(2), 433–459. https://doi.org/10.1007/s11101-020-09726-0.
Bocharova, O., Reshta, S., & Eshtokin, V. (2017). Toluene and benzyl alcohol formation in fruit juices containing benzoates. *Journal of Food Processing and Preservation, 41*(4), e13054. https://doi.org/10.1111/jfpp.13054.
Cardeal, Z. L., & Marriott, P. J. (2009). Comprehensive two-dimensional gas chromatography-mass spectrometry analysis and comparison of volatile organic compounds in Brazilian cachaça and selected spirits. *Food Chemistry, 112*(3), 747–755. https://doi.org/10.1016/j.foodchem.2008.06.057.
Cerny, C., & Herrmann, A. (2010). Chapter 9. Thermal Generation of Aroma-Active Volatiles in Food. In *The Chemistry and Biology of Volatiles* (pp. 231–252). John Wiley & Sons Ltd.
Chen, E., Song, H., Li, Y.i., Chen, H., Wang, B., Che, X., … Zhao, S. (2020). Analysis of aroma components from sugarcane to non-centrifugal cane sugar using GC-O-MS. *RSC Advances, 10*(54), 32276–32289. https://doi.org/10.1039/D0RA05963C.
Clarke, H. J., O'Sullivan, M. G., Kerry, J. P., & Kilcawley, K. N. (2020). Correlating volatile lipid oxidation compounds with consumer sensory data in dairy based powders during storage. *Antioxidants, 9*(4), 338. https://doi.org/10.3390/antiox9040338.
Coelho, C., Brottier, C., Beuchet, F., Elichiry-Ortiz, P., Bach, B., Lafarge, C., & Tourdot-Maréchal, R. (2020). Effect of ageing on lees and distillation process on fermented sugarcane molasses for the production of rum. *Food Chemistry, 303*, 125405. https://doi.org/10.1016/j.foodchem.2019.125405.
Cui, H., Jia, C., Hayat, K., Yu, J., Deng, S., Karangwa, E., … Zhang, X. (2017). Controlled formation of flavor compounds by preparation and application of Maillard reaction intermediate (MRI) derived from xylose and phenylalanine. *RSC Advances, 7*(72), 45442–45451. https://doi.org/10.1039/C7RA09355A.
De Andrade, J. K., Komatsu, E., Perreault, H., Torres, Y. R., Da Rosa, M. R., & Felsner, M. L. (2016). In house validation from direct determination of 5-hydroxy-methyl-2-furfural (HMF) in Brazilian corn and cane syrups samples by HPLC-UV. *Food Chemistry, 190*, 481–486. https://doi.org/10.1016/j.foodchem.2015.05.131.
De Souza, M. D. C. A., Vásquez, P., Del Mastro, N. L., Acree, T. E., & Lavin, E. H. (2006). Characterization of cachaça and rum aroma. *Journal of Agricultural and Food Chemistry, 54*(2), 485–488. https://doi.org/10.1021/jf0511190.
Deed, R. C., Pilkington, L. I., Herbst-Johnstone, M., Miskelly, G. M., Barker, D., & Fedrizzi, B. (2019). A new analytical method to measure S-methyl-l-methionine in grape juice reveals the influence of yeast on dimethyl sulfide production during fermentation. *Journal of the Science of Food and Agriculture, 99*(15), 6944–6953. https://doi.org/10.1002/jsfa.9983.
Dudareva, N., Klempien, A., Muhlemann, J. K., & Kaplan, I. (2013). Biosynthesis, function and metabolic engineering of plant volatile organic compounds. *New Phytologist, 198*(1), 16–32. https://doi.org/10.1111/nph.2013.198.issue-110.1111/nph.12145.
Edris, A. E., Murkovic, M., & Siegmund, B. (2007). Application of headspace-solid-phase microextraction and HPLC for the analysis of the aroma volatile components of treacle and determination of its content of 5-hydroxymethylfurfural (HMF). *Food Chemistry, 104*(3), 1310–1314. https://doi.org/10.1016/j.foodchem.2006.10.033.
Esteki, M., Simal-Gandara, J., Shahsavari, Z., Zandbaaf, S., Dashtaki, E., & Vander Heyden, Y. (2018). A review on the application of chromatographic methods, coupled to chemometrics, for food authentication. *Food Control, 93*, 165–182. https://doi.org/10.1016/j.foodcont.2018.06.015.
Eyong, K. O., Kuete, V., & Efferth, T. (2013). Quinones and Benzophenones from the Medicinal Plants of Africa. In *Medicinal Plant Research in Africa* (pp. 351–391). Elsevier. https://doi.org/10.1016/B978-0-12-405927-6.00010-2.
Franitza, L., Granvogl, M., & Schieberle, P. (2016). Influence of the production process on the key aroma compounds of rum: From molasses to the spirit. *Journal of Agricultural and Food Chemistry, 64*(47), 9041–9053. https://doi.org/10.1021/acs.jafc.6b04046.
Franitza, L., Nicolotti, L., Granvogl, M., & Schieberle, P. (2018). Differentiation of Rums Produced from Sugar Cane Juice (Rhum Agricole) from rums manufactured from sugar cane molasses by a metabolomics approach. *Journal of Agricultural and Food Chemistry, 66*(11), 3038–3045. https://doi.org/10.1021/acs.jafc.8b00180.
Gao, X. L., Cui, C., Zhao, H. F., Zhao, M. M., Yang, L., & Ren, J. Y. (2010). Changes in volatile aroma compounds of traditional chinese-type soy sauce during moromi fermentation and heat treatment. *Food Science and Biotechnology, 19*(4), 889–898. https://doi.org/10.1007/s10068-010-0126-7.
Gao, K., Zhou, L., Bi, J., Yi, J., Wu, X., & Xiao, M. (2017). Research on the nonenzymatic browning reactions in model systems based on apple slices dried by instant controlled pressure drop drying. *Drying Technology, 35*(11), 1302–1311. https://doi.org/10.1080/07373937.2017.1319856.
Göncüoğlu Taş, N., & Gökmen, V. (2017). Maillard reaction and caramelization during hazelnut roasting: A multiresponse kinetic study. *Food Chemistry, 221*, 1911–1922. https://doi.org/10.1016/j.foodchem.2016.11.159.
Hammerbacher, A., Coutinho, T. A., & Gershenzon, J. (2019). Roles of plant volatiles in defence against microbial pathogens and microbial exploitation of volatiles. *Plant Cell and Environment, 42*(10), 2827–2843. https://doi.org/10.1111/pce:v42.1010.1111/pce:13602.
Heravi, M. M., Zadsirjan, V., Hamidi, H., & Tabar Amiri, P. H. (2017). Total synthesis of natural products containing benzofuran rings. *RSC Advances, 7*(39), 24470–24521. https://doi.org/10.1039/c7ra03551a.
Ishwarya, S. P., & Anandharamakrishnan, C. (2015). Spray-Freeze-Drying approach for soluble coffee processing and its effect on quality characteristics. *Journal of Food Engineering, 149*, 171–180. https://doi.org/10.1016/j.jfoodeng.2014.10.011.
Joye, I. J. (2018). Acids and bases in food. In *Encyclopedia of Food Chemistry* (pp. 1–9). Elsevier. https://doi.org/10.1016/B978-0-08-100596-5.21582-5.
Kanakaraju, Y., Uma, A., Vani, G., Kiran Kumari, P., Sridhar, S., & Umakanth, A. V. (2020). Evaluation of ethanol fermentation efficiency of sweet sorghum syrups produced by integrated dual-membrane system. *Bioprocess and Biosystems Engineering, 43*(7), 1185–1194. https://doi.org/10.1007/s00449-020-02313-9.
Lubes, G., & Goodarzi, M. (2017). Analysis of volatile compounds by advanced analytical techniques and multivariate chemometrics. *Chemical Reviews, 117*(9), 6399–6422. https://doi.org/10.1021/acs.chemrev.6b00698.
Maire, M., Rega, B., Cuvelier, M. E., Soto, P., & Giampaoli, P. (2013). Lipid oxidation in baked products: Impact of formula and process on the generation of volatile compounds. *Food Chemistry, 141*(4), 3510–3518. https://doi.org/10.1016/j.foodchem.2013.06.039.
Parker, J. K. (2015). Introduction to aroma compounds in foods. In *Flavour Development, Analysis and Perception in Food and Beverages* (pp. 3–30). Elsevier. https://doi.org/10.1016/B978-1-78242-103-0.00001-1.
Payet, B., Shum, A., Sing, C., & Smadja, J. (2005). Assessment of antioxidant activity of cane brown sugars by ABTS and DPPH radical scavenging assays: Determination of their polyphenolic and volatile constituents. *Journal of Agricultural and Food Chemistry, 53*, 10074–10079. https://doi.org/10.1021/jf0517703.
Quinn, B. P., Bernier, U. R., Geden, C. J., Hogsette, J. A., & Carlson, D. A. (2007). Analysis of extracted and volatile components in blackstrap molasses feed as candidate house fly attractants. *Journal of Chromatography A, 1139*(2), 279–284. https://doi.org/10.1016/j.chroma.2006.11.039.
Raseetha, S., Oey, I., Burritt, D. J., Heenan, S., & Hamid, N. (2013). Evolution of antioxidant enzymes activity and volatile release during storage of processed broccoli (Brassica oleracea L. italica). *LWT - Food Science and Technology, 54*(1), 216–223. https://doi.org/10.1016/j.lwt.2013.05.024.
Rizzi, G. P. (2008). The strecker degradation of amino acids: Newer avenues for flavor formation. *Food Reviews International, 24*(4), 416–435. https://doi.org/10.1080/87559120802306058.
Ruiz-Matute, A. I., Soria, A. C., Sanz, M. L., & Martínez-Castro, I. (2010). Characterization of traditional Spanish edible plant syrups based on carbohydrate GC–MS analysis. *Journal of Food Composition and Analysis, 23*(3), 260–263. https://doi.org/10.1016/j.jfca.2009.08.017.
Santos-Zea, L., Leal-Díaz, A. M., Jacobo-Velázquez, D. A., Rodríguez-Rodríguez, J., García-Lara, S., & Gutiérrez-Uribe, J. A. (2016). Characterization of concentrated agave saps and storage effects on browning, antioxidant capacity and amino acid content. *Journal of Food Composition and Analysis, 45*, 113–120. https://doi.org/10.1016/j.jfca.2015.10.005.
Sengun, I. Y., & Karabiyikli, S. (2011). Importance of acetic acid bacteria in food industry. *Food Control, 22*(5), 647–656. https://doi.org/10.1016/j.foodcont.2010.11.008.
Serafim, F. A. T., Pereira-Filho, E. R., & Franco, D. W. (2016). Chemical data as markers of the geographical origins of sugarcane spirits. *Food Chemistry, 196*, 196–203. https://doi.org/10.1016/j.foodchem.2015.09.040.
Sharma, M. D., Rautela, I., Sharma, N., Gahlot, M., & Koshy, E. P. (2015). GC-MM analysis of phytocomponents in juice sample of Indian Cane: Saccharum Barberi. *International Journal of Pharmaceutical Sciences and Research, 6*(12), 5147–5153. https://doi.org/10.13040/IJPSR.0975-8232.6(12).5147-53.
Silva, P., Freitas, J., Silva, C. L., Perestrelo, R., Nunes, F. M., & Câmara, J. S. (2017). Establishment of authenticity and typicality of sugarcane honey based on volatile profile and multivariate analysis. *Food Control, 73*, 1176–1188. https://doi.org/10.1016/j.foodcont.2016.10.035.
Silva, P., Silva, C. L., Perestrelo, R., Nunes, F. M., & Câmara, J. S. (2018). Fingerprint targeted compounds in authenticity of sugarcane honey - An approach based on chromatographic and statistical data. *LWT, 96*, 82–89. https://doi.org/10.1016/J.LWT.2018.04.076.
Stasiak-Różńska, L., & Płoska, J. (2018). Study on the use of microbial cellulose as a biocarrier for 1,3-dihydroxy-2-propanone and its potential application in industry. *Polymers, 10*(4), 438. https://doi.org/10.3390/polym10040438.
Sumby, K. M., Grbin, P. R., & Jiranek, V. (2010). Microbial modulation of aromatic esters in wine: Current knowledge and future prospects. *Food Chemistry, 121*(1), 1–16. https://doi.org/10.1016/j.foodchem.2009.12.004.
Suzuki, T., Kim, S.-J., Mukasa, Y., Morishita, T., Noda, T., Takigawa, S., … Matsuura-Endo, C. (2010). Effects of lipase, lipoxygenase, peroxidase and free fatty acids on volatile compound found in boiled buckwheat noodles. *Journal of the Science of Food and Agriculture, 90*(7), 1232–1237. https://doi.org/10.1002/jsfa.3958.
Tábua, M. C. M., Santiago, W. D., Magalhães, M. L., Ferreira, V. R. F., Brandão, R. M., Teixeira, M. L., … das Graças Cardoso, M. (2020). Identification of volatile compounds, quantification of glycerol and trace elements in distilled spirits produced in Mozambique. *Journal of Food Science and Technology, 57*(2), 505–512. https://doi.org/10.1007/s13197-019-04079-9.
Takahashi, M., Ishmael, M., Asikin, Y., Hirose, N., Mizu, M., Shikanai, T., … Wada, K. (2016). Composition, Taste, Aroma, and Antioxidant Activity of Solidified Noncentrifugal Brown Sugars Prepared from Whole Stalk and Separated Pith of Sugarcane (Saccharum officinarum L.). *Journal of Food Science, 81*(11), C2647–C2655. https://doi.org/10.1111/jfds.2016.81.issue-1110.1111/1750-3841.13531.
Tan, Z.-W., & Yu, A.-N. (2012). Volatiles from the Maillard reaction of L -ascorbic acid with L -glutamic acid/ L -aspartic acid at different reaction times and temperatures. *Asia-Pacific Journal of Chemical Engineering, 7*(4), 563–571. https://doi.org/10.1002/apj.v7.410.1002/apj.607.
Thompson, S. (2009). Microbiological spoilage of high-sugar products. In *Compendium of the Microbiological Spoilage of Foods and Beverages* (pp. 301–324). https://doi.org/10.1007/978-1-4419-0826-1_11.

Tian, J.-P., Ma, Z.-Y., Zhao, K.-G., Zhang, J., Xiang, L., & Chen, L.-Q. (2019). Transcriptomic and proteomic approaches to explore the differences in monoterpene and benzenoid biosynthesis between scented and unscented genotypes of wintersweet. *Physiologia Plantarum, 166*(2), 478–493. https://doi.org/10.1111/ppl.12828.

Tokitomo, Y., Kobayashi, A., & Yamanishi, T. (1984). Aroma components of fresh sugar cane juice. *Agricultural and Biological Chemistry, 48*(11), 2869–2870. https://doi.org/10.1271/bbb1961.48.2869.

Ubeda, C., Callejón, R. M., Hidalgo, C., Torija, M. J., Mas, A., Troncoso, A. M., & Morales, M. L. (2011). Determination of major volatile compounds during the production of fruit vinegars by static headspace gas chromatography-mass spectrometry method. *Food Research International, 44*(1), 259–268. https://doi.org/10.1016/j.foodres.2010.10.025.

Ubeda, C., Kania-Zelada, I., del Barrio-Galán, R., Medel-Marabolí, M., Gil, M., & Peña-Neira, Á. (2019). Study of the changes in volatile compounds, aroma and sensory attributes during the production process of sparkling wine by traditional method. *Food Research International, 119*, 554–563. https://doi.org/10.1016/j.foodres.2018.10.032.

Wang, L.u., Deng, W., Wang, P., Huang, W., Wu, J., Zheng, T., & Chen, J. (2020). Degradations of aroma characteristics and changes of aroma related compounds, PPO activity, and antioxidant capacity in sugarcane juice during thermal process. *Journal of Food Science, 85*(4), 1140–1150. https://doi.org/10.1111/1750-3841.15108.

Wang, Y., Li, Y., Yang, J., Ruan, J., & Sun, C. (2016). Microbial volatile organic compounds and their application in microorganism identification in foodstuff. *TrAC - Trends in Analytical Chemistry, 78*, 1–16. https://doi.org/10.1016/j.trac.2015.08.010.

Wang, C., Lv, S., Wu, Y., Lian, M., Gao, X., & Meng, Q. (2016). Study of aroma formation and transformation during the manufacturing process of Biluochun green tea in Yunnan Province by HS-SPME and GC-MS. *Journal of the Science of Food and Agriculture, 96*(13), 4492–4498. https://doi.org/10.1002/jsfa.7663.

Wang, L., Wang, P., Deng, W., Cai, J., & Chen, J. (2019). Evaluation of aroma characteristics of sugarcane (Saccharum officinarum L.) juice using gas chromatography-mass spectrometry and electronic nose. *LWT, 108*, 400–406. https://doi.org/10.1016/j.lwt.2019.03.089.

Xu, Y., Luo, Z., Charles, M. T., Rolland, D., & Roussel, D. (2017). Pre-harvest UV-C irradiation triggers VOCs accumulation with alteration of antioxidant enzymes and phytohormones in strawberry leaves. *Journal of Plant Physiology, 218*, 265–274. https://doi.org/10.1016/j.jplph.2017.09.002.

Yang, H. F., Wang, S. L., Yu, S. J., Zeng, X. A., & Sun, D. W. (2014). Characterization and semiquantitative analysis of volatile compounds in six varieties of sugarcane juice. *International Journal of Food Engineering, 10*(4), 821–828. https://doi.org/10.1515/ijfe-2014-0105.

Yu, X., Zhao, M., Hu, J., Zeng, S., & Bai, X. (2012). Influence of pH on the formation and radical scavenging activity of volatile compounds produced by heating glucose with histidine/tyrosine. *European Food Research and Technology, 234*(2), 333–343. https://doi.org/10.1007/s00217-011-1644-0.

Zacaroni, L. M., de Sales, P. F., Cardoso, M. D. G., Santiago, W. D., & Nelson, D. L. (2017). Response surface optimization of SPME extraction conditions for the analysis of volatile compounds in Brazilian sugar cane spirits by HS-SPME-GC-MS. *Journal of the Institute of Brewing, 123*(2), 226–231. https://doi.org/10.1002/jib.410.

Zhou, D., Sun, Y., Li, M., Zhu, T., & Tu, K. (2019). Postharvest hot air and UV-C treatments enhance aroma-related volatiles by simulating the lipoxygenase pathway in peaches during cold storage. *Food Chemistry, 292*, 294–303. https://doi.org/10.1016/j.foodchem.2019.04.049.